polarimeter. *Planck*, for example, was only able to map 10 nearby clouds to a similar level of detail [110]. This large sample of clouds is crucial because dust polarization observations are sensitive to only the magnetic field projected on the plane of the sky, and therefore polarization maps will look very different for molecular clouds observed at different viewing angles. *By observing thousands of molecular clouds PICO will determine the role of magnetic fields in star formation as a function of cloud age and mass.*

• **Formation of Magnetized Molecular Clouds from the Diffuse Interstellar Medium** Structure formation in the diffuse ISM is a key area of study motivating observations across the electromagnetic spectrum. PICO's observations will complement recently completed high-dynamic-range neutral hydrogen (HI) surveys, such as HI4PI [122] and GALFA-HI [123], as well as planned surveys of interstellar gas, most prominently with the Square Kilometer Array (SKA) and its pathfinders. One of the open questions in diffuse structure formation is how gas flows within and between phases of the ISM. A planned all-sky absorption line survey with SKA-1 will increase the number of measurements of the ISM gas temperature by several orders of magnitude [124]. Quantitative comparisons of the ISM temperature distribution from SKA-1 and estimates of the magnetic field strength and coherence length scale from PICO will elucidate the role of the magnetic field in ISM phase transitions.

A comprehensive understanding of the magnetized diffuse ISM is challenging because of its diverse composition, its sheer expanse, and the multi-scale nature of the physics that shapes it. To understand how matter and energy are exchanged between the diffuse and dense media, it is essential to measure the properties of the magnetic field over many orders of magnitude in column density. PICO is unique in its ability to do this in the diffuse ISM. *Planck* achieved measurements of the diffuse sky at 60′ resolution, resulting in $\sim$30,000 independent measurements of the magnetic field direction in the diffuse ISM. With 1.1′ resolution PICO will expand the number of independent polarization measurements in the diffuse ISM to $\sim$86,000,000. This will allow us to robustly characterize turbulent properties like M_A across a previously unexplored regime of parameter space.

Galactic Legacy Science

PICO will also produce legacy datasets that will revolutionize our understanding of how magnetic fields influence physical processes ranging from planet formation to galaxy evolution. For 10 nearby clouds ($d < 500$ pc) PICO will resolve magnetic fields on the crucial 0.1 pc size scale associated with dense cores and filaments, and observe how the magnetic fields on these scales directly influence the formation structure of cores. By comparing the orientation of the core-scale magnetic field with respect to the orientation and sizes of protoplanetary disks, PICO will directly test whether there is evidence that magnetic breaking inhibits the growth of protoplanetary disks [125, 126].

On larger scales, PICO's tens of millions of independent measurements of magnetic field orientation will allow us to directly probe magnetized turbulence and study how magnetic fields are generated through a combination of turbulence and large scale gas motions [127]. Key processes in the diffuse ISM, including heat transport [128], streaming of cosmic rays [129], and magnetic reconnection [130] are dramatically dependent on the level of magnetization.

Finally, PICO observations will create detailed magnetic-field maps of approximately 70 nearby galaxies, with more than 100 measurements of magnetic field direction per galaxy. These observations will be used to study the turbulence on galactic scales, determine whether the magnetic fields

Table 2: **Cosmological Legacy Science**

Catalog	Impact	Science
1. Proto-Clusters	Discover $\sim$50,000[a] mm/sub-mm proto-clusters distributed over the sky and back to $z \sim 4.5$.	Probe the earliest phases of cluster evolution, well beyond the reach of other instruments; test the formation history of the most massive virialized halos; investigate galaxy evolution in dense environments.
	Current knowledge: *Planck* data expected to yield a few tens.	
2. Strongly Lensed Galaxies	Discover 4500[a] highly magnified dusty galaxies across redshift.	Gain unique information about the physics governing early, $z \simeq 5$, galaxy evolution, taking advantage of magnification and extra resolution enabled by gravitational lensing; learn about dark-matter sub-structure in the lensing galaxies.
	Current knowledge: 13 sources confirmed in *Planck* data; few hundred candidates in *Herschel*, SPT and ACT data.	
4. Polarized Point Sources	Detect 2000[b] radio and several thousand dusty galaxies in polarization.	Give information on the jets of extragalactic sources, close to their active nuclei. Determine the large-scale structure of magnetic fields in dusty galaxies. Determine the importance of polarized sources as a foreground for CMB polarization science.
	Current knowledge: $\sim$20 radio sources (from *Planck*, selected at 30 GHz); $\sim$200 (ground, up to 100 GHz; 1 polarization measurement of a dusty galaxy.	

[a] Confusion (not noise) limited
[b] Noise and confusion limited

of the Milky Way in the diffuse ISM are consistent with other galaxies, and directly study how interaction between large-scale magnetic fields, turbulence, and feedback from previous generations of star formation affect galaxy evolution and star-formation efficiency.

2.3 Cosmological Legacy Surveys

2.3.1 Early phases of galaxy evolution

PICO will have a crucial role in providing answers to major, still open issues on galaxy formation and evolution. Which are the main physical mechanisms shaping the galaxy properties [136, 137]: in situ processes, interactions, mergers, or cold flows from the intergalactic medium? How do feedback processes work? To settle these issues we need direct information on the structure and the dynamics of high-z galaxies. But these are compact, with typical sizes of 1–2 kpc [138]), corresponding to angular sizes of 0.1–0.2 arcsec at $z \simeq 2$–3. Thus they are hardly resolved even by ALMA and by HST. If they are resolved, high enough SNR per resolution element are achieved only for the brightest galaxies, which are probably not representative of the general population.

Strong gravitational lensing provides a solution to these problems. PICO will detect galaxies whose flux densities are boosted by large factors (see the right panel of Fig. 12). Since lensing conserves the surface brightness, the effective angular size is stretched on average by a factor $\mu^{1/2}$, where μ is the gravitational magnification, thus substantially increasing the resolving power. A spectacular example are ALMA observations of the strongly lensed galaxy PLCK_G244.8+54.9 at $z \simeq 3.0$ with $\mu \simeq 30$ [139]. ALMA observation with a 0.1″ resolution reached the astounding spatial resolution of $\sim$60 pc, substantially smaller than the size of Galactic giant molecular clouds. Other high-z galaxies spatially resolved thanks to gravitational lensing with less extreme magnifications are reported by Dye et al. [140], and others [141, 142].

Cañameras et al. [139] have also obtained CO spectroscopy, measuring the kinematics of the

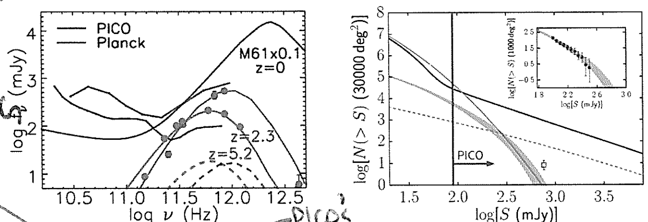

Figure 12: **Left panel**: Example spectral energy distributions (SEDs) of dusty star-forming galaxies detectable by PICO, compared with its point-source detection limits (black line) and with the *Planck* 90% completeness limits (red line [131]). PICO will detect nearby galaxies, like M 61 (magenta), whose SED was scaled down by a factor of 10, and high-z strongly lensed galaxies, like SMM J2135-0102 (blue) at $z = 2.3$ [132] and HLSJ091828.6+514223 (orange) at $z = 5.2$ [133]. The dashed lines are corrected for lensing magnification. **Right panel**: Integral counts at 500 μm (600 GHz) of unlensed, low-z (black) and strongly lensed, high-z (orange) star-forming galaxies based on fits of *Herschel* counts (inset [134]), also shown are predicted radio source counts (green). The PICO detection region (right of vertical red line) will yield a factor of 1000 increase in strongly lensed galaxies relative to Planck (yellow square), and $\sim$ 50,000 proto-clusters (blue) [135].

molecular gas with an uncertainty of 40–50 km/s. This spectral resolution makes possible a direct investigation of massive outflows driven by AGN feedback at high z. In this way Spilker et al. [143] were able to detect a fast (800 km/s) molecular outflow due to feedback in a strongly lensed galaxy at $z = 5.3$. The outflow carries mass at a rate close to the SFR and can thus remove a large fraction of the gas available for star formation.

Herschel surveys have demonstrated that, at the PICO detection limit at 500 μm (600 GHz), about 25% of all detected extragalactic sources are strongly lensed; for comparison, at optical/near-IR and radio wavelengths, were intensive searches have been carried out for many years, the yield is of only 0.1%, i.e. more than two orders of magnitude lower [144]. To add to the extraordinary sub-mm bonanza, the selection of strongly lensed galaxies detected by sub-mm surveys is extremely easy because of their peculiar sub-mm colors – see the left panel of Fig. 12 – resulting in a selection efficiency close to 100% [145].

A straightforward extrapolation of the *Herschel* counts to the much larger area covered by PICO shows that its surveys will yield $\sim$ 4,500 strongly lensed galaxies with a redshift distribution peaking at $2 \lesssim z \lesssim 3$ [134] but extending up to $z > 5$ see the left panel of Fig. 12. If objects like the $z = 5.2$ strongly lensed galaxy HLSJ091828.6+514223 exist at higher redshifts, they will be detectable by PICO up to $z > 10$.

An intensive high spectral and spatial resolution follow-up campaign of such a large sample will be challenging but also extremely rewarding since it will allow a giant leap forward towards the understanding of the processes driving early galaxy evolution, in addition to opening many other exciting prospects both on the astrophysical and on the cosmological side (cf., e.g., ref. [144]). The PICO all-sky surveys will select the brightest objects in the sky, maximizing the efficiency of the effort.

2.3.2 Early phases of cluster evolution

PICO will open a new window for the investigation of early phases of cluster evolution, when their member galaxies were actively star forming but the hot IGM was not necessarily in place. In this phase, traditional approaches to cluster detection (X-ray and SZ surveys searches for galaxy red sequences) work only for the more evolved objects; indeed these methods have yielded only a handful of confirmed proto-clusters at $z \gtrsim 1.5$ [146]. *Planck* has demonstrated the power of low-resolution surveys for the study of large-scale structure [147] but its resolution was too poor to detect individual proto-clusters [135]. Studies of the high-z 2-point correlation function [108, 135] and *Herschel* images of the few sub-mm bright protoclusters detected so far, at z of up to 4 [148–150] all of which will be detected by PICO indicate sizes of $\simeq 1'$ for the cluster cores, nicely matching the PICO FWHM at the highest frequencies.

PICO will detect many tens of thousands of these objects this is the blue line in the right-hand panel of Fig. 12 as peaks in its sub-mm maps, in addition to the evolved ones, detected by the SZ effect. This will constitute a real breakthrough in the observational validation of the formation history of the most massive dark-matter halos traced by clusters, a crucial test of models for structure formation. Follow-up observations will characterize the properties of member galaxies, probing the galaxy evolution in dense environments and shedding light on the complex physical processes driving it.

2.3.3 Additional products of PICO surveys

PICO will also yield a complete census of cold dust, available to sustain star formation in the nearby universe, by detecting tens of thousands galaxies mostly at $z \lesssim 0.1$. Its statistics will allow us to investigate the distribution of such dust as a function of galaxy properties (morphology, stellar mass, etc.).

Moreover, PICO will increase by orders of magnitude the number of blazars selected at sub-mm wavelengths and will determine the SEDs of many hundreds of them up to 800 GHz and up to $z > 5$. Blazar searches are the most effective way to sample the most massive BHs at high z because of the Doppler boosting of their flux densities. Its surveys of the largely unexplored mm/sub-mm spectral region will also offer the possibility to discover new transient sources [151] or events, such as blazar outbursts.

PICO will also make a giant leap forward in the determination of polarization properties of both radio sources and of dusty galaxies over a frequency range where ground-based surveys are impractical or impossible. Thanks to its high sensitivity, it will detect in polarization both populations over a substantial flux-density range, determining directly, for the first time number counts in polarized flux density and allowing an accurate correction for their contamination of CMB maps.

The anisotropy of the cosmic infrared background (CIB), produced by dusty star-forming galaxies in a wide redshift range, is an excellent probe of both the history of star formation and the link between galaxies and dark matter across cosmic time. The *Planck* collaboration derived values of the star-formation rate up to redshifts $z \sim 4$ [152–154]. It was quantified in [155] that the increased SNR and frequency coverage enabled by PICO will enable an order of magnitude improvement on the statistical errors on these parameters. Similar improvement will be achieved in constraining $M_{\rm eff}$, the galaxy halo mass that is most efficient in producing star-formation activity. PICO extra-

[4]More high-z proto-clusters have been found targeting the environment of tracers of very massive halos, such as radio-galaxies, QSOs, sub-mm galaxies. These searches are however obviously biased.

Characteristic	Ground	Balloon	Space
Sky coverage	Partial from single site	Partial from single flight	Full
Frequency coverage	70 GHz inaccessible[a] $\nu \geq 300$ GHz unusable limited atmospheric windows	70 GHz inaccessible[a] otherwise, almost unlimited	Unrestricted
Angular resolution at 150 GHz[b]	1.5' with 6 m telescope	6' with 1.5 m telescope	6' with 1.5 m telescope
Detector Noise	265 microK rt(s)[c]	124 microK rt(s)[c]	36 microK rt(s)[c]
Integration time	Unlimited	Weeks to a Month	Continuous, for years
Accessibility, repairability	Good	None. Multiple flights possible.	None

[a] 70 GHz is the frequency at which large angular scale *B*-mode Galactic emissions have a minimum.
[b] We give representative approximate telescope aperture values. Significantly larger apertures for balloons and in space result in higher mass, volume, and cost.
[c] Noise equivalent temperature: timestream-based median at 95 GHz from BICEP3 [156]; pre-flight expectation at 94 GHz from SPIDER [157]; at 90 GHz from PICO CBE.

Table 3: Relative characteristics of ground, balloon, and space platforms for experiments in the CMB bands.

frequencies and increased sensitivity to galactic dust polarization will provide enhanced means to separate the largely unpolarized CIB from polarized galactic dust, the limiting factor towards more extended reliable legacy CIB maps.

2.4 Complementarity with Other Surveys and with Sub-Orbital Measurements

2.4.1 Complementarity with Astrophysical Surveys in the 2020s

PICO has strong complementarity with forthcoming surveys. Here we summarize areas of synergy that have been mentioned in a number of earlier sections.

There is no known way to achieve any cosmological constraint on the sum of the neutrino mass $\sigma(\sum m_\nu) < 25$ meV without improving *Planck*'s measurement of the optical depth τ. In particular, this applies to all methods that rely on comparing low-redshift structures with the amplitude of the CMB at high redshift, such as galaxy clustering, weak lensing, or cluster counts. PICO therefore complements all efforts that probe the late-time structure of the Universe; combining PICO with these low-redshift observations extends the scientific reach of all these experiments well beyond what they could achieve on their own.

Reconstructing the CMB lensing ϕ map on very large angular scales, $L < 20$, requires exquisite control of systematic uncertainties over a large sky fraction, with sufficient angular resolution to perform the lensing reconstruction, and with breadth in frequency band to robustly separate Galactic emissions (see Section 2.5). PICO will provide these, complementing ground-based CMB lensing reconstructions that typically observe a smaller sky fraction, with a smaller number of frequency bands, and without access to the largest angular scales. As discussed on page 13, PICO will robustly measure the lensing signal with a power spectrum SNR larger than 10 *per mode* on very large scales. Such high-significance CMB lensing measurements on the very largest scales will be useful when combined with measurements of galaxy clustering from LSST, Euclid, and SPHEREx (if selected), to search for local primordial non-Gaussianity via its scale-dependent effect on galaxy bias; see Section 2.2.1.

2.4.2 Complementarity with Sub-Orbital Measurements

Since the first CMB measurements, more than 50 years ago, important observations have been made from the ground, from balloons, and from space. Each of the CMB satellites flown to date (COBE, WMAP, and *Planck*) has relied crucially on technologies and techniques that were first proved on ground and balloon flights, making these also crucial to the success of PICO. The phenomenal success of, and the immense science outcomes produced by, past space missions is a direct consequence of their relative advantages, as listed in Table 3. In every respect, with the exception of repairability, space has the advantage. These advantages used to come with higher

relative costs. However, with the advent of massive ground-based experiments this balance shifts; the costs for a CMB experiment planned for the next decade are squarely within the cost window of this Probe. We can thus point to the following general guidelines for the next decade.

When the entire sky is needed, as for fluctuations on the largest angular scales, space is by far the most suitable platform, and for the search for the IGW signal it is absolutely necessary. When broad frequency coverage is needed, space will be required to reach the ultimate limits set by astronomical foregrounds. As Figures 1 and 13 demonstrate, Galactic emission overwhelms the IGW signal on the largest angular scales, and they are dominant even at high ℓ, potentially limiting the process of delensing that is necessary for reaching levels of $r \lesssim 0.001$. The stability offered in space cannot be matched on any other platform and translates to superb control of systematic uncertainties. There is a broad consensus within the CMB community that for levels of $r \lesssim 0.001$ the challenges in the measurement are the ability to control systematic uncertainties and to remove Galactic emissions; modern focal-plane arrays, like the one employed by PICO, have ample raw sensitivity. The PICO goal of $\sigma(r) = 1 \times 10^{-4}$ is beyond the reach of ground observations. However, for science requiring higher angular resolution, such as observations of galaxy clusters with 1 arcmin resolution at 150 GHz, the ground has a clear advantage. An appropriately large aperture on the ground will also provide high-resolution information at lower frequencies, which may be important for separating Galactic emissions at high ℓ. A recommended plan for the next decade is therefore to pursue a space mission, and complement it with an aggressive ground program that will overlap in ℓ space, and will add science at the highest angular resolution, beyond the reach of a space mission.

Balloon observations have been exceedingly valuable in the past. They co-lead discoveries of the temperature anisotropy and polarization, provided proving grounds for the technologies enabling the success of COBE, WMAP and *Planck*, and trained the scientists that then led NASA's space missions. There are specific areas for which balloon missions can continue to play an important role, despite their inherently limited observing time. Balloon payload can access frequency bands above 280 GHz; currently there are no plans for any ground program to conduct observations at higher frequencies. These frequency bands will provide important, and perhaps critical information about polarized emission by Galactic dust, a foreground that is currently known to limit knowledge of the CMB signals. With flights above 99% of the atmosphere, balloon-borne observations are free from the noise induced by atmospheric turbulence, making them good platforms for observations of the low-ℓ multipoles, and for characterizing foregrounds on these very large angular scales. From a technology point of view, the near-space environment is the best available for elevating detector technologies to TRL6; and balloon-platforms continue to be an excellent arena for training the scientists of tomorrow.

2.5 Signal Separation

Diffuse Milky Way emissions dominate the sky's polarized intensity on the largest angular scales; see Figures 1 and 13. Polarized radiation arises primarily from the synchrotron emission of energetic electrons spiralling in the magnetic field of our own Galaxy, and from thermal emission from elongated interstellar dust grains. Although the levels of these foreground emissions decrease with decreasing angular scales, they can still be considerably brighter than the IGW peak around $\ell = 80$ when averaging over 60% of the sky. In fact, even in the cleanest, smaller patches of the sky, far from the galactic plane and thus relatively low in galactic emissions, their levels are expected to be substantial relative to the IGW for $r \lesssim 0.01$, and dominate it for $r \lesssim 0.001$. Separating the cosmological and Galactic emission signals (also called foreground separation) together with control of systematic uncertainties are *the* challenges facing any next-decade experiment attempting to reach these levels of constraints on r.

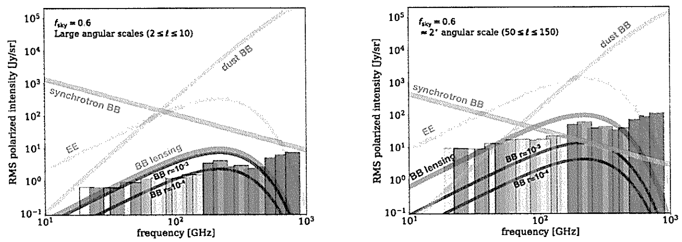

Figure 13: Polarization BB spectra of Galactic synchrotron and dust, compared to CMB polarization EE and BB spectra of different origins for two values of r and for two ranges of angular scales: large $\ell \leq 10$ corresponding to the reionization peak (left panel) and intermediate $50 \leq \ell \leq 150$ corresponding to the recombination peak (right panel). The location and sensitivity of the 21 PICO frequency channels is shown as vertical bands. The color scheme is explained in Section 3.2.

The foreground-separation challenge would be easily surmountable if the Galactic emissions were precisely characterized, or were known to have simple, fittable spectral emission laws. But neither is true. To first order, the spectrum of Galactic synchrotron emission, arising from free electrons spiraling around Galactic magnetic fields, can be modeled as a power law $I_{\rm sync} \propto \nu^{\alpha}$, with $\alpha \simeq -1$ (in brightness units). The spectrum of Galactic dust emission, arising from emission by Galactic dust grains, can be modeled as $I_{\rm dust} \propto \nu^{\beta} B_{\nu}(T_{\rm dust})$, where $\beta \simeq 1.6$, $T_{\rm dust} \gtrsim 19$ K, and $B_{\nu}(T)$ is the Planck function; this is referred to as 'modified black body emission'. If those models were exact, then in principle, an experiment that had 6 frequency bands could determine the three emission parameters as well as the three amplitudes corresponding to that of dust, synchrotron, and the CMB. However, recent observations have shown that neither emission law is universal, that spectral parameters vary with the region of sky [158–160], and thus that the analytic forms and parameter values given above are valid only as averages across the sky. Also, while both emission laws are well-motivated phenomenological descriptions, the fundamental physics of emissions from grains of different materials, sizes and temperatures, and of electrons spiraling around magnetic fields implies that these laws are not expected to be exact, nor universal.

Additional polarized foregrounds may exist. 'Anomalous microwave emission' (AME) is observed at mm wavelengths, spatially correlated with thermal dust emission but with intensity peaked at frequencies near 30 GHz. While not known to be polarized, even a small (0.1%) fractional polarization would be appreciable for $\sigma(r) \lesssim 0.001$. Astrophysical emission from CO lines at mm wavelengths, and even small polarization of radio and infrared sources at shorter wavelengths could also complicate polarized signal separation [161, 162].

PICO will dramatically improve sensitivity to inflationary B-modes. The improved sensitivity requires concurrent improvements in foreground separation. Simple foreground models, suitable for the current generation of CMB measurements, will fail at the higher PICO sensitivity. For

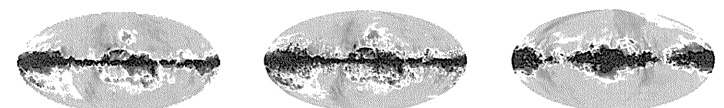

Figure 14: Foregrounds maps: Planck real sky (left) at 143 GHz, models at 155 GHz from PySM (middle) [168] and Galactic MHD simulations (right).

example, the Planck modified blackbody model assumes that interstellar dust emits at a single temperature, which is clearly an approximation to the more complicated emission along lines of sight spanning hundreds of pc. Several publications have demonstrated that fitting complicated temperature profiles using a simple one- or two-temperature model will bias the fitted CMB signal at levels $\delta r \lesssim 10^{-3}$, large compared to the PICO goal [163–167].

Foreground uncertainties, and the level of fidelity required in their characterization, also compel a transition in the way we assess and forecast the performance of a future experiment. We can no longer impose specific models upon the data; rather, the data collected should provide information to constrain Galactic emissions with sufficient accuracy. Two broad techniques are available. Parametric models use the frequency dependence of the data in each line of sight to determine the effective frequency dependence of foreground emission. Since the CMB spectrum is well determined, measurements with sufficiently broad frequency coverage can distinguish foreground emission from the CMB component by their different spectral dependences. Non-parametric techniques, in contrast, rely on the fact that CMB emission is uncorrelated with the foregrounds and use both spatial and frequency correlations within a spatial/frequency data cube to separate CMB from foreground components. Simulated data assess the efficacy of both techniques as a function of increasing complexity for the assumed foreground emission.

To investigate the capacity of PICO to address this foreground-separation problem, we use the approach that has become the 'gold standard' in the community. In this approach we simulate sky maps that are constrained by available data, but otherwise have a mixture of foreground properties. We 'observe' these maps just like a realistic experiment will do, and then apply foreground-separation techniques to separate the Galactic and CMB emission. We also provide forecasts using other techniques that use analytic calculations to estimate the efficacy of foreground separation, or others in which the simulated sky map is assumed to have specific Galactic emission models, which are then being fitted.

2.5.1 PICO Foreground Separation Methodology

For assessing the efficacy of foreground separation with PICO we used 9 different full-sky models. All models were broadly consistent with available data and uncertainties from WMAP and *Planck*. The range of models included one test case that had a very simple realization of foregrounds, and others with varying degree of complexity including spectral parameters varying spatially and along the line of sight, anomalous microwave emission up to 2% polarized, dust polarization that rotates slightly as a function of frequency because of projection effects, or dust spectral energy distribution that depart from a simple modified blackbody. All foreground maps were generated at native resolution of 6.8 arcmin pixels [169]. They were generated using PySM and/or PSM codes [168, 170]. Distinctly different realizations of the sky are allowed by current data, as demonstrated by Figure 14.

For each of the 9 models we added CMB signals in both intensity and polarization matching

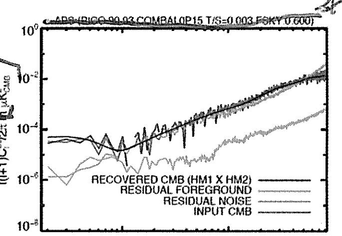

Figure 15: The power spectrum of residual *BB* foregrounds (green) has lower level than both the input CMB (blue) and the recovered CMB (red), which match well each other and the underlying cosmological model (black) after foreground separation with the NILC algorithm. This exercise assumed use of 60% of the sky.

a ΛCDM universe. The *BB*-lensing signal matched the level of 85% delensing forecasted for PICO. Each of these sky models had 100 different realization of the PICO CBE noise levels; 50 realizations had no IGW signal and 50 others had a level of $r = 0.003$. The sky models were analyzed with a variety of techniques which were based on the two broad categories described above.

Analytic forecasts were based on a Fisher information matrix approach [171] and included foreground separation using a parametric maximum-likelihood approach, assuming the foreground spectral indices are constant on patches of size 15 degrees across.

2.5.2 Results and Discussion

There is evidence that at levels of $r \simeq 0.001$ the combination of PICO's sensitivity and broad frequency coverage are efficacious in foreground removal. Figure 15 shows a result from the gold-standard process described above for one of the sky models and with an input IGW of $r = 0.003$. Residual foregrounds are below the cosmological signal over the important low-ℓ range, where foregrounds are strongest. The residual spectra would likely be lower when analysis is carried out on only 50 or 40% of the sky, rather than the 60% used here.

Our results validate the need for a broad frequency coverage with a strong lever arm on Galactic emission outside of the primary CMB bands. Figure 16 shows that removing several of PICO's frequency bands, particularly those that monitor dust and synchrotron at high and low frequencies, respectively, significantly biases the extracted *BB* power spectrum, particularly at the lowest values.

There is other evidence that PICO could reach its stated target of $\sigma(r) = 0.0001$. Map-based simulations that were carried out for the forthcoming CMB-S4 experiment have shown that it can reach levels of $\sigma(r) = 0.0005$ in small, 3%-size, clean patches of the sky. The analysis only used frequencies up to 300 GHz. In principle, even smaller patches of 1-2% size are sufficient and preferable for attaining as low $\sigma(r)$ as possible. The PICO noise level per sky pixel is similar to that of CMB-S4, but PICO will have *full* sky coverage and thus access to *all* the clean patches available. Data from *Planck* indicate that there are 10 patches as clean, or cleaner than those used for the CMB-S4 analysis, indicating that PICO's $\sigma(r)$ could be 3 times more stringent. This scaling is very conservative because it only assumes CMB-S4's much narrower breadth of frequency coverage and its bands; it neglects PICOs much stronger rejection of foregrounds with 21 bands and up to 800 GHz. We note that if there is a detection of the IGW signal with $r = 0.001$, PICO will make it with high significance in multiple independent patches of the sky.

Results from the Fisher-based analytic calculations give $\sigma(r) = 9 \times 10^{-5}$, and indicate a very

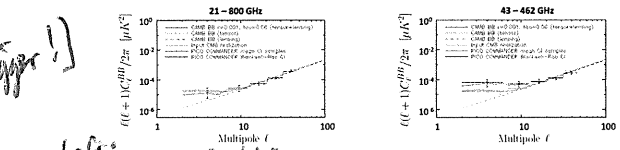

Figure 16: Foreground removal with all of PICO's 21 frequency bands (left panel) recovers the input CMB (green) without any bias (red) using the Commander algorithm on the *Planck* sky model (with 4 deg pixels, and 50% sky fraction). Running the same algorithm on the same sky without several of the lowest and highest bands (right panel) produces an output spectrum (red) that is biased relative to the input (green) at low ℓ multipoles. The bias would be interpreted as higher value of r relative to the model input (solid black) with $r = 0.001$ (dots) and lensing (dash).

small foreground residual with an $r_{eff} = 9 \times 10^{-7}$.

While our results are encouraging, as they suggest that PICO's frequency coverage and sensitivity will be adequate for this level of r, more work should be invested to gain complete confidence. This work includes running numerous realizations of different sky models, and analyzing them with various techniques; optimizing sky masks; and using combination of techniques to handle large, intermediate, and small angular scale foregrounds differently.

2.6 Systematic Uncertainties

Some of the PICO science goals attempt to detect extremely faint signals. The most ambitious one is to reach the signals characterizing an inflationary gravity wave with $r \lesssim 0.001$, with a B-mode polarization peak signal $\lesssim 10$nK in amplitude at $\ell = 80$. It has long been recognized that exquisite control of systematic uncertainties will be required for any experiment attempting to reach these levels, and it is widely accepted that the stability provided aboard a space platform makes it best suited to control systematic uncertainties compared to other platforms. This is one of the most compelling reasons to observe the CMB from space. As WMAP and *Planck* demonstrated, an L2 orbit offers excellent stability as well as the flexibility in the choice of scan strategy. PICO takes advantage of an L2 orbit, using a rotating spacecraft (at 1 rpm) whose spin axis precesses with a 10 hour period, thus scanning the sky in a way that is crosslinked on many time scales and at many angles, without interference from the Sun, Earth, or Moon, thus reducing the effects of low frequency excess noise without additional modulation. The redundancy of observations allows the checking of consistency of results and an improved ability to calibrate and to correct systematic errors in post-processing analysis.

A rich literature investigates the types of systematic errors due to the environment, the instrumentation, observation strategies, and data analysis that confound the polarization measurement by creating a bias or an increased variance [172–174]. Every measurement to date has reached a systematic error limit, and have advanced many sophisticated techniques to mitigate systematics, finding both new technological solutions and new analysis techniques. As an example, the BICEP systematics limited it to $r = 0.1$ [175] while through additional effort within the program, BICEP2 achieved a systematics limit of $r = 6 \times 10^{-3}$ [176]). In the near term, the ground-based and suborbital CMB community will continue to develop new techniques in handling systematics, particularly in developing the CMB-S4 project.

All prior on-orbit measurements of CMB polarization were limited by systematic errors until an in-depth study of the systematics was performed and the post-processing data analysis suppressed them[21, 43, 177]. Particularly we note Fig. 3 of [21], which quantifies Planck's systematic error limits on the polarization power spectral measurements. Recently studied space missions, such as EPIC-IM, LiteBird and *CORE*, have placed systematic error mitigation at the forefront of the case for their mission and have developed tools and strategies for estimating and mitigating these[178–180].

Systematics are coupled with the spacecraft scan strategy, and the details of the data analysis pipeline. Thus, end-to-end simulation of the experiment is an essential tool, including realistic instabilities and non-idealities of the spacecraft, telescope, instrument, and folding in data post-processing techniques used to mitigate the effects.

2.6.1 List of Systematics

The systematic errors faced by PICO can be categorized into three broad categories: 1) Intensity-to-polarization leakage, 2) stability, and 3) straylight, and are listed in Table 4. These were prioritized for further study using a risk factor incorporating the working group's assessment of how mission-limiting the effect is, how well these effects are understood by the community and whether mitigation techniques exist.

The three highest risk systematic errors were studied further and are discussed in subsections below. The PICO team used simulation and analysis tools developed for Planck[181] and *CORE*, adapting them for PICO.

Name	Risk	Effect	
Leakage			
Polarization Angle Calibration	5	$E \to B$	See Sect. 2.6.2.
Bandpass Mismatch	4	$T \to$P, $E \to B$	
Beam mismatch	4	$T \to$P, $E \to B$	See Sect. 2.6.2
Time Response Accuracy and Stability	4	$T \to$P, $E \to B$	
Readout Cross-talk	4	spurious P	
Chromatic beam shape	4	spurious P	
Gain mismatch	3	$T \to$P	
Cross-polarization	3	$E \to B$	
Stability			
Gain Stability	5	$T \to$P, $E \to B$	See Sect. 2.6.3
Pointing jitter	3	$T \to$P, $E \to B$	
Straylight			
Far Sidelobes	5	spurious P	See Sect. 2.6.4.
Other			
Residual correlated noise (cosmic ray hits)	3	increased variance	

Table 4: Systematic errors expected in PICO's measurement of CMB polarization. Each source of systematic errors was given a rating of the risk that a given systematic error will dominate the B-mode measurement. A risk level of 5 indicates that a systematic effect is highly significant because it is design-driving, has limited past experiments, and/or is not well understood. Risk level of 4 indicates a systematic that is either known to be large but is understood reasonably well or a smaller effect that requires precise modeling. Risk level of 3 indicates that we expect the effect to be small, but it isn't necessarily well understood enough that modeling it should be done in detail in a mission Phase A. This study investigated the systematics with risk levels of 5 via simulations.

2.6.2 Absolute polarization angle calibration

CMB polarization can be rotated due to (1) a birefringent primordial Universe, or a Faraday rotation due a primordial magnetic field [182], (2) birefringent foregrounds, or interaction with the Galactic magnetic field, (3) systematic effects in the instrument, and in particular an error on the direction of polarization measured by each detector. While the first two sources create a rotation that may depend on scale, position and/or frequency, the latter depends mainly on the detector.

A rotation α of the direction of polarization mixes the Q and U Stokes parameters via $Q \pm iU \longrightarrow e^{\mp i2\alpha}(Q \pm iU)$ and thus mixes the the power spectra and their correlations as illustrated in Fig. 17.

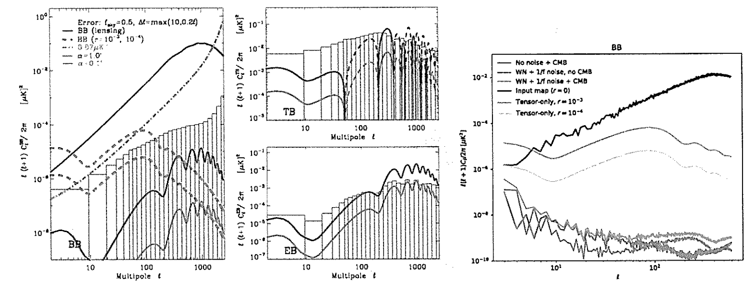

Figure 17: Effect of a rotation of the angle of polarization, assuming the Planck 2018 Λ-CDM best fit model [42] with $\tau = 0.054$ and expected PICO noise performance, assuming perfect delensing.

The most recent constraints on cosmological birefringence Planck Collaboration [183] were limited by uncertainties on the detector orientations. In Planck, the detectors were characterized pre-launch to ±0.9° (rel.) ±0.3° (abs.) [184]. For PICO, the relative rotation of the detectors will be measured to a few 0.1′ using the CMB, but the overall rotation is unlikely to be known pre-launch to better than Planck. Known polarized sources, such as the Crab Nebula, are not characterized well enough independently to serve as calibrators; Aumont et al. [185] show that the current uncertainty of 0.33° ±20′ on the Crab polarization orientation, limits a B-mode measurement to $r \sim 0.01$, far from PICO's target.

In the absence of other systematics and foregrounds, a polarization rotation error α of $10'$ degrades the error bar of r by 30%, while EB, TB and BB spectra can measure a rotation α at 3σ when $\alpha = 0.07, 0.2$ and $0.9'$ respectively on perfectly delensed maps, and $0.25, 0.9$ and $4.5'$ on raw maps.

In principle, the technique of using the TB and EB spectra can detect and measure a global polarization rotation error at levels ($0.1'$) below those affecting r measurements in BB ($> 1'$). However, a future mission should simulate additional aspects such as delensing, the interaction with foregrounds, and $1/f$ noise in simulating and assessing the impact of an angle calibration error.

2.6.3 Gain Stability

Photometric calibration is the process of converting the raw output of the receivers into astrophysical units via the characterization of the *gain factor* $G(t)$, which we allow to vary with time. In space, $G(t)$ can be measured with the dipole. For the PICO concept study, we evaluated the impact of noise in the estimation of $G(t)$ using the tools developed for the Planck/LFI instrument and the CORE mission proposal. The quality of the estimate depends on the noise level of the receivers, but also on the details of the scanning strategy. To analyze the impact of calibration uncertainties on PICO, we performed the following analysis. (1) We simulated the observation of the sky, assuming four receivers, the nominal scanning strategy, and $1/f$ noise. The simulated sky contained CMB anisotropies, plus the CMB dipole. (2) We ran the calibration code to fit the dipole against the raw data simulated during step 1. (3). We again simulated the observation of the sky, this time using the values of G computed during step 2, which contain errors due to the presence of noise and the CMB signal.

The presence of large-scale Galactic emission features can bias the estimation of calibration factors. Ideally, a full data-analysis pipeline would pair the calibration step with the component-separation step, following a schema similar to Planck/LFI's legacy data processing [186]: the calibration code is followed by a component-separation analysis, and these two steps are iterated until the solution converges.

Results of the simulation (neglecting foregrounds) are shown as power spectrum residuals in Fig. 17. We estimate the gain fluctuations to better than 10^{-4} solving for the gain every 40 hours (4 precession periods). The scanning strategy employed by PICO allows for a much better calibration than Planck, thanks to the much faster precession.

2.6.4 Far-Sidelobe Pickup

Measurement of each detector's response to signals off axis, which tend to be weak (–80dB less than the peak response) but spread over a very large solid angle, is difficult to do pre-launch, and may not even be done accurately after launch. Nonetheless, this far sidelobe can couple bright Galactic signal from many tens of degrees off-axis and confuse it with polarized signal from the CMB off the Galactic plane. To evaluate this systematic error, GRASP software[5] was used to compute the PICO telescope's response over the full sky. The computed full-sky beams showed features peaking at about -80 dB of the on-axis beam. This full-sky beam was convolved with a polarized Galactic signal and a one-year PICO mission scan using the simulation pipeline and preliminarily shows that the far sidelobe pickup must be calculated accurately down to the 90 dB level in order to be removed from the measured B-mode signal to a level that does not appreciably increase the variance on the B-mode power measurement.

2.6.5 Key Findings

Properly modeling, engineering for, and controlling the effects of systematic errors in a next-generation CMB probe is critical. As of today, we conclude that there is a clear path to demonstrate that state-of-the-art technology and data processing can take advantage of the L2 environment and control systematic errors to a level that enables the science goals of PICO. In particular we note:

- The raw sensitivity of the instrument should include enough margin that data subsets can independently achieve the science goals. This allows testing of the results in the data analysis

[5] https://www.ticra.com

and additional data cuts, if needed.

- In a PICO mission, a physical optics model of the telescope should be developed, enabling full-sky beam calculations, which should be validated as much as possible on the ground. This will be needed to characterize and remove far-sidelobe pickup seen during the mission.
- NASA's support of ground-based and suborbital CMB missions will mitigate risk to a future space mission as PICO by continuing to develop analysis techniques and technology for mitigation of systematic errors.
- In a PICO mission's phase A, a complete end-to-end system-level simulation software facility would be developed to assist the team in setting requirements and conducting trades between subsystem requirements while realistically accounting for post-processing mitigation. Any future CMB mission is likely to have similar orbit and scan characteristics to those of PICO, thus there is an opportunity for NASA and the CMB community to invest in further development of this capability now.

2.7 Measurement Requirements

The set of physical parameters and observables that derive from the PICO science objectives place requirements on the depth of the mission, the fraction of sky the instrument scans, the frequency range the instrument probes and the number of frequency bands, the angular resolution provided by the reflectors, and the specific pattern with which PICO will observe the sky. We discuss each of these aspects.

• Depth We quantify survey depth in terms of the RMS fluctuations that would give a signal-to-noise ratio of 1 on a sky pixel that is 1 arcminute on a side. Depth in any frequency band is determined by detector sensitivity, the number of detectors in the focal plane, the sky area covered, and the duration of the mission. The science objective driving the depth requirement is SO1; the search for the IGW signal which requires a depth of 0.87 μK · arcmin. This requirement is a combination of the low-level of the signal, the need to separate the various signals detected in each band, and the need to detect and subtract systematic effects to anticipated levels. The CBE value is 0.61 μK · arcmin coming from a realistic estimate of detector noise, and giving 40% margin on mission performance.

• Sky Coverage There are several science goals driving a full-sky survey for PICO. The term 'full sky' refers to the entire area of sky available after separating other astrophysical sources of confusion. In practice this implies an area of 50-70% of the full sky for probing non-Galactic signals, and the rest of the sky for achieving the Galactic science goals. The main goals are

(1) Probing the optical depth to the epoch of reionization (STM SO5) requires full-sky coverage as the signal peaks in the *EE* power spectrum on angular scales of 20 to 90 degrees. Measuring this optical depth to limits imposed by the statics of the small number of available ℓ modes is crucial for minimizing the error on the neutrino-mass measurement.

(2) If $r \neq 0$, the *BB* power spectrum due to IGW (STM SO1) has local maxima on large angular scales (20 to 90 degrees, $2 \leq \ell \leq 10$), and around 1 degree ($\ell \simeq 80$). A detection would strongly benefit from confirmation at *both* angular scales – a goal that is beyond the capabilities of ground-based instruments – and, for the $\ell = 80$ peak, *in several independent patches of the sky*, a goal PICO will achieve, but that is currently not planned for any next-decade instrument.

(3) The PICO constraint on N_{eff} (STM SO4) requires a determination of the *EE* power spectrum

to limits imposed by the statics of available ℓ modes. Full sky coverage is required to achieve this limit.
(4) Achieving the neutrino mass limits (STM SO3), giving two independent 4σ constraints on the minimal sum of 58 meV, requires a lensing map, and cluster counts from as large a sky fraction as possible.
(5) PICO's survey of the Galactic plane and regions outside of it is essential to achieving its Galactic structure and star formation science goals (SO6, 7).

• **Frequency Bands** The multitude of astrophysical signals that PICO will characterize determine the frequency range and number of bands that the mission uses. The GW signal peaks in the frequency range between 30 and 300 GHz. However, Galactic signals, which are themselves signals PICO strives to characterize, are a source of confusion for the GW. The Galactic signals and the GW are separable using their spectral signature. Simulations indicate that 21 bands, each with $\approx$25% bandwidth, that are spread across the range of 20–800 GHz can achieve the separation at the level of fidelity required by PICO.

Characterizing the Galactic signals, specifically the make-up of Galactic dust (SO7), requires spectral characterization of galactic dust in frequencies between 100 and 800 GHz.

• **Resolution** Several science objectives require an aperture of 1.5 m and the resolution per frequency listed in Table 1. To reach $\sigma(r) = 1 \times 10^{-4}$ we will need to 'delens' the E- and B-mode maps, as describe in Sections 2.2.1 and 2.2.2. Delensing is enabled with a map that has a native resolution of 2-3 arcminutes at frequencies between 100 and 300 GHz. Similar resolution is required to achieve the constraints on the number of light relics (SO4), which will be extracted from the EE power spectrum at multipoles $100 \lesssim \ell \lesssim 2500$. The process of delensing may be affected by other signals, primarily the signal due to Galactic dust. It is thus required to map Galactic dust to at least the same resolution as at 300 GHz. Higher resolution is mandated by SO6 and 7, which require resolution of 1 arcminute at 800 GHz. We have thus chosen to implement diffracted-limited resolution between 20 and 800 GHz.

• **Sky Scan Pattern** Control of polarization systematics uncertainties at anticipated levels is enabled by (1) making I, Q, and U Stokes parameters maps of the entire sky from each independent detector; and (2) by enabling sub-percent absolute gain calibration of the detectors through observations of the CMB dipole. With these requirements we chose a sky scan pattern that enables each detector to scan a given pixel of the sky in multitude of directions, satisfying requirement (1). The scan we chose also gives strong CMB dipole signals in every rotation of the spacecraft throughout the lifetime of the mission, satisfying requirement (2).

References

[1] Committee for a Decadal Survey of Astronomy and Astrophysics. *New Worlds, New Horizons in Astronomy and Astrophysics*. National Academy Press, 2010.

[2] K. Array, BICEP2 Collaborations, :, P. A. R. Ade, Z. Ahmed, R. W. Aikin, K. D. Alexander, D. Barkats, S. J. Benton, C. A. Bischoff, J. J. Bock, R. Bowens-Rubin, J. A. Brevik, I. Buder, E. Bullock, V. Buza, J. Connors, J. Cornelison, B. P. Crill, M. Crumrine, M. Dierickx, L. Duband, C. Dvorkin, J. P. Filippini, S. Fliescher, J. Grayson, G. Hall, M. Halpern, S. Harrison, S. R. Hildebrandt, G. C. Hilton, H. Hui, K. D. Irwin, J. Kang, K. S. Karkare, E. Karpel, J. P. Kaufman, B. G. Keating, S. Kefeli, S. A. Kernasovskiy, J. M. Kovac, C. L. Kuo, N. A. Larsen, K. Lau, E. M. Leitch, M. Lueker, K. G. Megerian, L. Moncelsi, T. Namikawa, C. B. Netterfield, H. T. Nguyen, R. O'Brient, R. W. Ogburn, IV, S. Palladino, C. Pryke, B. Racine, S. Richter, A. Schillaci, R. Schwarz, C. D. Sheehy, A. Soliman, T. St. Germaine, Z. K. Staniszewski, B. Steinbach, R. V. Sudiwala, G. P. Teply, K. L. Thompson, J. E. Tolan, C. Tucker, A. D. Turner, C. Umilta, A. G. Vieregg, A. Wandui, A. C. Weber, D. V. Wiebe, J. Willmert, C. L. Wong, W. L. K. Wu, H. Yang, K. W. Yoon, and C. Zhang. BICEP2 / Keck Array x: Constraints on Primordial Gravitational Waves using Planck, WMAP, and New BICEP2/Keck Observations through the 2015 Season. *ArXiv e-prints*, October 2018.

[3] Planck Collaboration, R. Adam, P. A. R. Ade, N. Aghanim, M. Arnaud, J. Aumont, C. Baccigalupi, A. J. Banday, R. B. Barreiro, J. G. Bartlett, and et al. Planck intermediate results. XXX. The angular power spectrum of polarized dust emission at intermediate and high Galactic latitudes. *Astron. Astrophys.*, 586:A133, February 2016. doi: 10.1051/0004-6361/201425034.

[4] Uros Seljak and Matias Zaldarriaga. Signature of gravity waves in polarization of the microwave background. *Phys. Rev. Lett.*, 78:2054–2057, 1997. doi: 10.1103/PhysRevLett.78.2054.

[5] Marc Kamionkowski, Arthur Kosowsky, and Albert Stebbins. A Probe of primordial gravity waves and vorticity. *Phys. Rev. Lett.*, 78:2058–2061, 1997. doi: 10.1103/PhysRevLett.78.2058.

[6] Alan H. Guth. The Inflationary Universe: A Possible Solution to the Horizon and Flatness Problems. *Phys. Rev.*, D23:347–356, 1981. doi: 10.1103/PhysRevD.23.347. [Adv. Ser. Astrophys. Cosmol.3,139(1987)].

[7] Andrei D. Linde. A New Inflationary Universe Scenario: A Possible Solution of the Horizon, Flatness, Homogeneity, Isotropy and Primordial Monopole Problems. *Phys. Lett.*, 108B:389–393, 1982. doi: 10.1016/0370-2693(82)91219-9. [Adv. Ser. Astrophys. Cosmol.3,149(1987)].

[8] Andreas Albrecht and Paul J. Steinhardt. Cosmology for Grand Unified Theories with Radiatively Induced Symmetry Breaking. *Phys. Rev. Lett.*, 48:1220–1223, 1982. doi: 10.1103/PhysRevLett.48.1220. [Adv. Ser. Astrophys. Cosmol.3,158(1987)].